Digital Object Identifier: 10.1109/ULTSYM.2008.0170

Fully-Differential Mechanically-coupled PZT-on-Silicon Filters

Hengky Chandrahalim and Sunil A. Bhave
School of Electrical and Computer Engineering
Cornell University
Ithaca, USA

Ronald G. Polcawich, Jeff S. Pulskamp, Daniel Judy,
Roger Kaul and Madan Dubey
US Army Research Laboratory
Adelphi, USA

***Abstract*—This paper reports on the design of a 2-pole differential MEMS filter using mechanically-coupled overtone width-extensional resonators. The resonators and filters are fabricated in the 10 µm thick device layer of a SOI wafer and transduced by a 0.5 µm PZT (lead zirconate titanate) thin film deposited on the top surface of the wafer. A 206.3 MHz overtone width-extensional filter is demonstrated with 653 kHz bandwidth, -25 dB insertion loss (IL) and -62 dB stop-band rejection in air. Uncompensated temperature coefficient of frequency (TCF) of -16 ppm/°C and third-order input intercept point (IIP3) of +52.5 dBm are demonstrated by the filter. The piezoelectric response of the filter is controlled by varying the electric field across the PZT transducer. A 20 dB improvement in IL and 0.22% center frequency tuning resulted by applying 20 V DC tuning voltage.**

Keywords-RF MEMS; differential; filter; PZT; piezoelectric transduction; voltage tuning

I. INTRODUCTION

Frequency agile intermediate frequency (IF) filters with narrow bandwidth, excellent stop-band rejection and modest frequency trimming are necessary in multi-band radio technology such as the Army's Blue radio and Joint Tactical Radio Systems (JTRS). Aluminum Nitride (AlN) is the most favored material for fabrication of thin film BAW and contour-mode resonators and filters. There are certainly good reasons for it, such as the high acoustic velocity, the high quality factor (Q), and post-CMOS integration capability [1, 2]. However there are several motivations to seek new piezoelectric/ferroelectric transducers for resonators and filters. One is to avoid the large area and large thicknesses required for AlN resonators below 1GHz. At low frequencies, ferroelectrics like PZT are better suited as they avoid thick film requirements and reduce the area required for the filters. Furthermore, PZT exhibits larger coupling factors than AlN (a feature we have exploited for making large force PZT RF MEMS switches [3]). Finally, the polarization, capacitance, dielectric loss, and piezoelectric coefficient of PZT can be tuned by a superimposed DC electric field. The coupling coefficient is DC voltage dependent which is attractive for tunable IF resonators and filters [4].

PZT has been previously used for memory and MEMS Actuators/Robotics applications. Film bulk acoustic resonators made from PZT have been previously demonstrated having large coupling coefficient (k_t^2: 10-35%) but low quality factors (Q: 45 – 220) [4-6]. To overcome the low quality factor of PZT-only resonators, we have developed a novel fabrication technology by integrating PZT transduction with single-crystal silicon [7]. Since the mechanical energy in this class of resonators is retained in the single crystal silicon layer, the resonators and filters have higher quality factors and higher acoustic velocity compared to PZT-only counterparts (Q: 2000 – 4000). By applying a DC bias across the PZT transducer, the transducer coupling coefficient and filter center frequency can be tuned, enabling voltage-dependent dynamic voltage frequency tuning and trimming.

The most desirable properties of intermediate frequency channel-select filters in modern radios are high filter Q, small shape factor and excellent stop-band rejection. A closely packed dense array of MEMS filters on the same chip introduces large feed-through capacitance between the drive and sense electrodes, leading to poor stop-band rejection of the filter. The fully-differential PZT-on-silicon filter configuration cancels the feed-through capacitance and improves the stop-band floor of the filter.

II. MECHANICALLY-COUPLED OVERTONE WIDTH-EXTENSIONAL FILTER

The resonant frequency of vibration for contour mode resonators and filters is defined by lithography. Therefore, contour-mode filters are preferred for realizing multi-band and multi-frequency filters on a single-chip [2]. The width-extensional mode of a contour-mode resonator is given by:

$$f = \frac{n}{W}\sqrt{\frac{E}{\rho}} \tag{1}$$

where W is the width of the resonator, E and ρ are effective elastic modulus for 2D expansion and density of the resonator respectively, and n is the harmonic order. Higher frequency overtone modes of the width-extensional mode resonators are selectively excited by patterning electrodes in differential interdigitated configuration on top of the resonator [8].

Electrically-coupled filters using AlN overtone-mode resonators have been recently demonstrated with narrow-bandwidth and low *IL* [9]. However, the electrical losses in the shunt capacitors and the patterned ground-plane degrade the shape-factor of the filter. These losses are more severe in electrically-coupled differential lattice configurations. Mechanically-coupled devices demand smaller area since the coupling spring is small. Furthermore, they do not suffer from energy losses since the coupling spring is made of crystalline material and do not require extra device area to implement a differential configuration due to inherent mechanical inversion

available through the resonators [10]. To realize a two-pole mechanically-coupled filter, two resonators are coupled using a suspension spring as shown in Fig. 1. The length of the coupling spring is designed to be quarter acoustic-wavelength long to minimize mass-loading of the resonators. The width of the coupling spring then defines the stiffness of the coupling spring. The bandwidth (*BW*) of such a mechanically-coupled filter is given by:

$$BW = \frac{f_0}{k_{ij}} \cdot \frac{k_s}{k_r} \qquad (2)$$

where f_0 is the resonant frequency, k_s and k_r are the spring stiffness of the coupling spring and resonator respectively and k_{ij} is the filter coefficient from the filter cookbook [11].

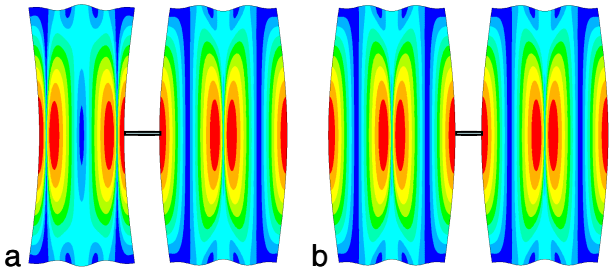

Figure 1. Ansys mode shape of a high overtone width-extensional filter. (a) Out-of-phase motion, (b) In-phase motion.

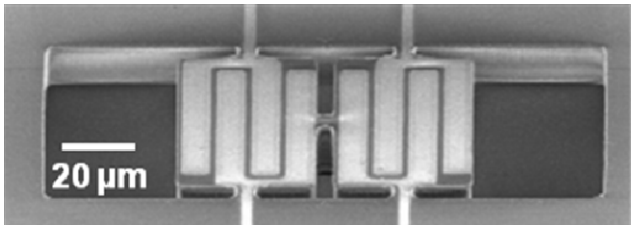

Figure 2. SEM image of a high overtone mechanically-coupled width-extensional filter with differential electrodes.

III. Fabrication Process

The resonators and filters are fabricated in a 5-mask SOI process and follow similar steps as reported in [7]. We started with a p-type low-resistivity SOI wafer with a 10 µm device layer and grow 50 nm thick thermal oxide for electrical isolation between the piezoelectric transducer and the high-*Q* mechanical silicon layer. Next, a stack of 100 nm platinum, 0.5 µm PZT [12] and 100 nm of platinum was deposited. The top platinum layer was patterned by ion milling to define the interdigitated transducer electrodes and signal pads. This was followed by wet-etching of the PZT film to open ground contact holes to the bottom metal layer. We then defined the resonators and filters by successive patterning PZT, bottom-metal, thermal-oxide, 10 µm thick silicon device layer and buried oxide, stopping the etch on the silicon substrate. Finally, we defined release holes in thick photoresist and perform a XeF_2 etch of the silicon substrate to undercut and release the composite PZT-Silicon resonators and filters. The final release step is the key innovation — it provides protection of PZT layer during etch and performs a gentle front-side release that alleviates the need for backside DRIE. SEM image of the fabricated device is shown in Fig. 2.

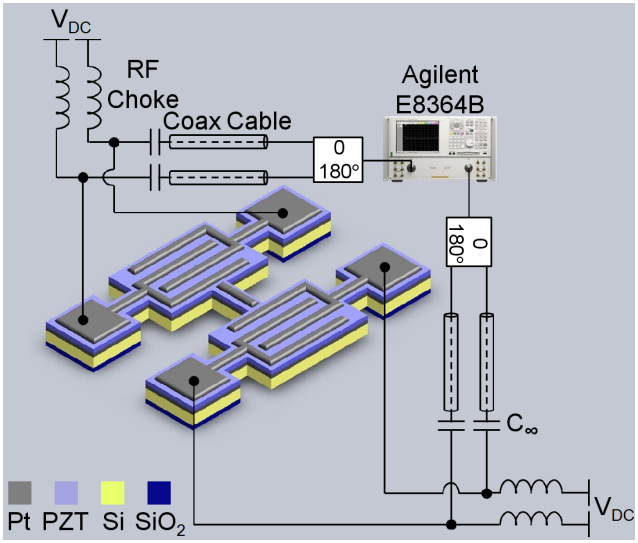

Figure 3. Testing configuration for a 2-pole mechanically-coupled differential filter.

IV. Measurement Results

A. *Frequency response of an overtone width-extensional filter*

We characterized the 2-pole fully-differential mechanically coupled filter as illustrated in Fig. 3. The fully-differential configuration enables us to cancel feedthrough capacitances between drive and sense electrodes thereby improving the stop-band floor of the filter. While the working principle of a differential filter is straightforward, experimental technique and configuration is significantly more challenging. The filter was characterized on a Cascade microwave probe station using GSGSG probes and a 4-port Agilent N5230A network analyzer. Bias-Ts from Minicircuits were used to apply independent DC bias tuning voltages to the 4 electrodes. The setup (including the Bias-Ts and up to the GSGSG probes) is calibrated using differential SOLT calibration on a Cascade ISS substrate. After performing a complete parametric 4-port frequency sweep, we measure the fully-differential transmission response by plotting the following mathematical function [13]:

$$S_{DD21} = 0.5 \times [S_{21} - S_{23} - S_{41} + S_{43}] \qquad (3)$$

Fig. 4 shows the frequency response when only one input electrode was used to actuate the filter and one output electrode was used to sense the motional current. The response of the 2-port measurement shows that the filter exhibits 20 dB stop-band rejection at 20 V DC bias. The low value of stop-band rejection is caused by the capacitive feedthrough current between input and output terminals.

Fig. 5 shows the differential filter response as we apply DC bias voltages to the electrodes. The DC bias voltage not only improves the piezoelectric coupling coefficient (via poling of

the ferroelectric domains), but also increases the Young's modulus of the PZT film. The improvement in the coupling coefficient improves the insertion loss by 5 dB and improves the stop-band rejection from 20 dB to 35 dB. The increase in Young's modulus of the PZT film, increases the effectively acoustic velocity of the PZT-Silicon composite resonator, thereby increasing the resonant frequency. The result is a 0.22% increase in filter center frequency for 20 V_{DC} applied bias. We intentionally did no attempt to correctly impedance match the filter in order to highlight the coupling coefficient and center frequency tuning capability of a PZT-Si resonator.

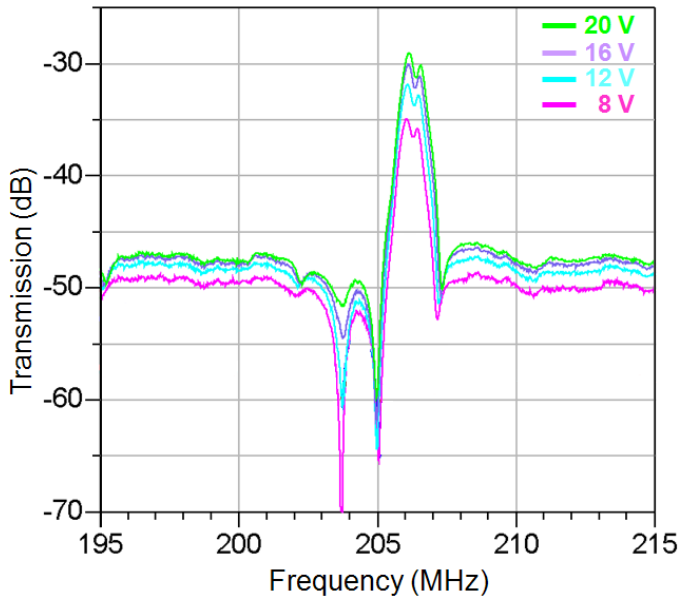

Figure 4. 2-port measured transmission of a high overtone 2-pole width-extensional filter with V_{DC} = 8-20V in 4V increment step.

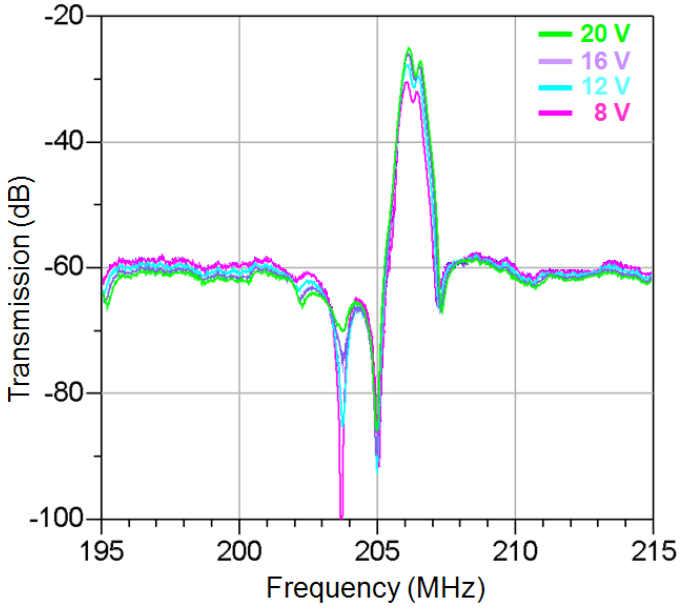

Figure 5. 4-port measured transmission of a high overtone 2-pole width-extensional filter with V_{DC} = 8-20V in 4V increment step.

B. *Hysteresis effect in the PZT-on-silicon filter*

Hysteresis of PZT can cause an undesirable resonance frequency drift in the filter. By integrating PZT transduction with 10 µm thick SOI the frequency shift due to hysteresis can be minimized. The hysteresis effect in PZT-on-silicon is translated into very minor frequency drifts as shown in Fig. 6. This effect can be simply compensated with the DC tuning.

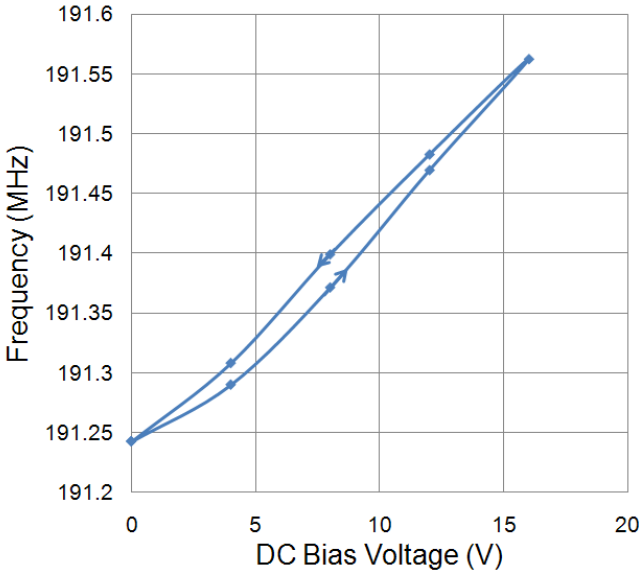

Figure 6. Measured frequency shifts in PZT-on-silicon filter due hysteresis effect in PZT (Δ_f Max = 0.014%).

C. *Linearity in the PZT-on-silicon filter*

The immunity of the resonators to the third-order intermodulation distortion (IM_3) was characterized by using two-tones technique. Two interferer signals f_1 and f_2 separated Δ_f away from each other are generated by the signal generators to excite the in-band IM_3 at $f_C = 2f_1 - f_2$. Both interferer signals were excited in the bandpass region of the filter with Δ_f = 400 kHz. By integrating PZT transduction with SCS, the non-linear behavior of PZT can be suppressed because the vibrating structure is dominated by silicon that has a superior acoustic linearity. The filter demonstrated the third-order input intercept point (IIP_3) of +52.5 dBm as shown in Fig. 7.

D. *Temperature coefficient of frequency (TCF)*

All the measurement results demonstrated up to this point have shown the filter performances at room temperature and pressure. Several targeted applications of this filter, however, operate at environments with wide range of temperature fluctuations. Thus filters with high insensitivity to temperature variations are highly desirable. Temperature characterization was performed by placing the filter on the Cascade probe station with temperature control stage. Frequency responses were recorded while the device was cooled down to -20 °C and heated up to 100 °C. The filter with different DC bias voltages was characterized over the whole temperature range of operation and exhibits TCF between -16 to -21 ppm/°C. These

values are comparable to AlN transduced resonators and filters and quartz crystals used in time-keeping applications for handsets [14]. Measured temperature coefficient of frequency of the filter with V_{DC} = 8 - 16 V in 4V increment is shown in Fig. 8.

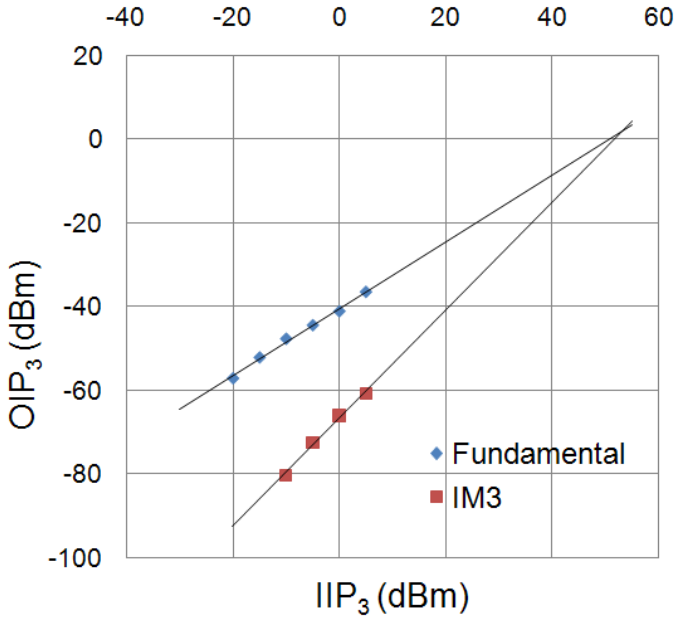

Figure 7. Measured third-order input intercept point (Δ_f = 400 kHz) of the filter demonstrates IIP_3 of 52.5 dBm.

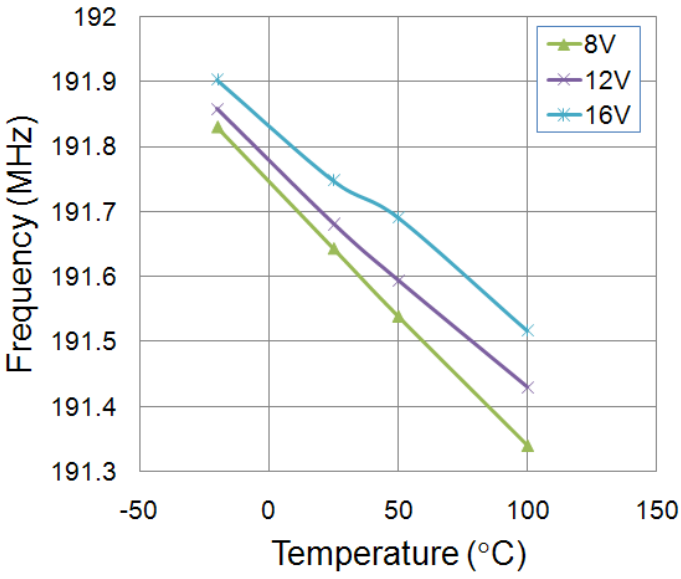

Figure 8. Measured temperature coefficient of frequency of the filter with V_{DC} = 8-20V in 4V increment step demonstrates TCF of -16 to -21 ppm/°C.

V. Conclusion

We have developed PZT-on-SOI RF MEMS technology and demonstrated linear and temperature stable mechanically-coupled intermediate frequency filters that are immune to hysteresis effect of PZT. Composite PZT-Silicon resonators demonstrate significant enhancement in *Q* compared to PZT-only devices. Differential mechanical coupling enables fabrication of small-footprint and high stop-band rejection filters. The DC voltage dependent tuning capability of the filters can be used to enable post-fabrication frequency trimming and tuning.

Acknowledgment

The authors wish to acknowledge the assistance and support of Joel Martin and Brian Power of General Technical Services and Richard Piekarz from the ARL for their hard work with device fabrication.

References

[1] R. C. Ruby, A. Barfknecht, C. Han, Y. Desai, F. Geefay, G. Gan, M. Gat, and T. Verhoeven, "High-Q FBAR filters in a wafer-level chip-scale package," *IEEE International Solid-State Circuits Conference (ISSCC) 2002*, 3-7 Feb. 2002 Page(s):184-185 vol.1.

[2] G.Piazza, P.J. Stephanou, M.B.J. Wijesundara and A.P. Pisano, "Single-chip multiple-frequency filters based on contour-mode aluminum nitride piezoelectric micromechanical resonators," *IEEE Transducers'05*, 5-9 June 2005 Page(s):2065-2068 Vol. 2.

[3] Ronald G. Polcawich, Daniel Judy, Jeffrey S. Pulskamp, Susan Trolier-McKinstry, and Madan Dubey, "Advances in Piezoelectrically Actuated RF MEMS Switches and Phase Shifters," *IEEE/MTT-S International*, 3-8 June 2007 Page(s):2083-2086.

[4] M. Schreiter, R. Gabl, D. Pitzer, R. Primig and W. Wersing , "Electro-acoustic hysteresis behaviour of PZT thin film bulk acoustic resonators," *Journal of the European Ceramic Society*, v 24, n 6, June, 2004, p 1589-1592.

[5] John D. Larson III, Stephen R. Gilbert, and Baomin Xu, "PZT material properties at UHF and microwave frequencies derived from FBAR measurements," *Ultrasonics Symposium 2004*, 23-27 Aug. 2004 Page(s):173 - 177 Vol.1

[6] J. Conde and P. Muralt, *IEEE Transactions on Ultrasonics, Ferroelectrics and Frequency Control*, Vol. 55, n6, pp. 1373-1379, 2008.

[7] Hengky Chandrahalim, Sunil A. Bhave, Ronald Polcawich, Jeff Pulskamp, Daniel Judy, Roger Kaul and Madan Dubey, "Influence of silicon on quality factor, motional impedance, and tuning range of PZT-transduced resonators," *Solid State Sensor, Actuator and Microsystems Workshop*, Hilton Head Island, SC, pp. 360-363, 2008.

[8] Gavin K. Ho, Reza Abdolvand, and Farrokh Ayazi, "High-order composite bulk acoustic resonators," *IEEE MEMS 2007*, 21-25 January 2007. pp. 781-794.

[9] Chengjie Zuo, Nipun Sinha, Marcelo B. Pisani, Carlos R. Perez, Rashed Mahameed and Gianluca Piazza, "Channel-select RF MEMS filters based on self-coupled AlN contour-mode piezoelectric resonators," *Ultrasonics Symposium 2007*, 28-31 Oct. 2007.

[10] Sunil A. Bhave, Di Gao, Roya Maboudian, and Roger T. Howe, "Fully-differential poly-SiC Lame mode resonator and checkerboard filter," *IEEE MEMS 2005*, 30 Jan.-3 Feb. 2005 Page(s):223 - 226.

[11] Anatol I. Zverev, *Handbook of Filter Synthesis*. New York John Wiley & Sons, 1967.

[12] K. Budd, S. Dey, and D. Payne, " Sol-gel processing of PbTiO3, PbZrO3, PZT, and PLZT thin films," *Brit. Ceram. Proc, 36*, 107-121, 1985.

[13] Kun Wang, Michael Frank, Paul Bradley, Richard Ruby, William Mueller, Andrew Barfknecht, and Moshe Gat, "FBAR Rx filters for handset front-end modules with wafer-level packaging," *IEEE Ultrasonics Symposium 2003*, 5-8 Oct. 2003 Page(s):162 - 165 Vol.1

[14] G. Piazza, P. J. Stephanou and A.P. Pisano, "Piezoelectric aluminum nitride vibrating contour-mode MEMS resonators," JMEMS 15 (6) 2006, pp. 1406-1418.